

## Combining Neural Networks and Global Gabor Features in a Hybrid Face Recognition System

Eng. Catalin-Mircea Dumitrescu

Department of System Engineering  
Politehnica University of Bucharest  
Bucharest, Romania  
dumitrescu.catalin.m@gmail.com

Acad. Ioan Dumitrache

Department of System Engineering  
Politehnica University of Bucharest  
Bucharest, Romania  
ioan.dumitrache@acse.pub.ro

**Abstract**— Face recognition is the preferred mode of identification by humans: it is natural, robust and non-intrusive. Face recognition is the most effective and natural technique to identify a person, since it is the same as the way human does and there is no need to use any special equipment. In this paper, a novel face recognition approach is proposed based on Global Facial Features and Neural Networks.

The Global Facial Features are extracted using a Gabor wavelet filter; by applying it on the whole image. The face registration is done with the help of Neural Networks and the classification with a nearest-neighbor classifier.

The hybrid algorithm was tested on multiple face databases, ORL, Caltech, Yale and Yale B, in order to validate the face recognition rate. The results show that the new face recognition algorithm out-performs the conventional methods such as global Gabor face recognition with PCA in term of recognition rate.

**Keywords**- Face Recognition, Global Facial Features, Neural Networks, ORL (Olivetti Research Laboratory)

### I. INTRODUCTION

A biometric marker (trait) can be defined as an anatomic attribute (*face, fingerprint, DNA, iris etc.*) or behavioral characteristic (*voice, signature etc.*), which can be used by itself, or in combination with other traits, in order to identify / recognize a person, a prerequisite in many applications such as control, defense, banking and so on.

The advances registered by *Information and Communication Technology* domain (*ICT*) and mobile devices, combined with the decrease in production costs of biometric sensors, stimulated the research and development of *Automated Biometric Recognition Systems (ABRS)*.

The biometric market analysis, presented by Acuity Market Intelligence in 2016 [1], predicted that the *ABRS* market in mobile biometric context will grow from 6.5 billion \$, in 2016, to 50.6 billion \$ in 2022. Annually, approximately 1.37 trillion biometrically secured payment and non-payment transactions will generate \$18.3 billion in annual authentication fees.

A *Facial Recognition System (FRS)* is a computer application capable of identifying an individual from a digital image or video frame.

*Face recognition* represents a *non-intrusive* and *user-friendly biometric security technique*; it is the least invasive authentication method available, requiring almost

no-user interaction. *Face recognition* methods can be used for verification and identification of unknown individuals with applications in security, surveillance, general identity verification (access control systems), criminal justice systems, and image database investigations [2]. In addition to the classic applications, there are many emerging fields that can benefit from *FRS*, such as human-computer interfaces and e-services, including e-home, tele-shopping, tele-banking and machine-to-human (*M2H*) communication.

*Being a natural fit for smart mobile devices, facial biometrics* have been integrated with consumer electronics in order to facilitate user authentication, replacing the usage of passwords. Using data from cameras, even a 100\$ mobile phone can be unlocked as soon as the user is in front of it.

*FRS* solutions can be used to authenticate the right of electronic access to *Collaborative Decision Support Systems (CDSSs)*. Under the influence of the new technologies, *CDSSs* have evolved from few people located in a “*decision room*” to an unlimited number of participants over a distributed architecture [3], thus, the identification of the participants has become an important topic.

Face recognition combined with *Artificial Intelligence (AI)* is also set to change the face of the Advertising Sector. The retailer Tesco intends to install hi-tech OptimEyes [4] screens in order to deliver targeted ads to customers after identifying the age range and gender of waiting customers.

*Face recognition techniques* include three main categories based on the face data acquisition technique: methods that operate on intensity images, methods that deal with video sequences and methods that require other sensory data such as 3D information or infra-red images [2].

By using face recognition in conjunction with many other biometrics, such as speech, iris, fingerprint, the quality of recognition and identification can be improved.

The biggest problem of facial recognition systems is that the recognition rate is heavily affected by changes in illumination, pose and facial expressions. Thus, is difficult to design a system that handles all these problems and is simple enough.

The most popular global facial feature extraction methods are *Principal Component Analysis (PCA)* [5], *Linear Discriminant Analysis (LDA)* [6], *Independent Component Analysis (ICA)* [7], *Discrete Random Transform* [8] and *Gabor Wavelet* [9] [10]. In [9], the authors presented a new facial feature extraction based on

**Gabor wavelets** and AdaBoost. In [10], the use of **Gabor wavelets** for efficient face representation is described.

In this paper, we propose a new hybrid algorithm for face recognition, which uses **Gabor Wavelet filters** for feature extraction and a **Neural Network** architecture to solve the classification problem. First, we extract the **Global Gabor features** from the whole image (frontal face images), and then for each subject a **Neural Network model** is trained. In the recognition phase, the classifier compares the features vector of the sample image with the facial models that are stored in the database and selects the model with the maximum likelihood value.

The paper is organized as follows: a short review of the **Gabor wavelet filter**, in Section 2. In Section 3, the **Neural Networks** used for subject modelling are presented. The proposed algorithm is described in Section 4. In Section 5, experimental results are shown. Finally, the conclusions are presented in Section 6.

## II. GABOR WAVELET FILTERS

**Gabor functions** (*wavelet*) or *atoms* have been used in many different fields, since their introduction in 1946 by the Hungarian-born engineer Denis Gabor [11]. **Gabor functions are one of the most important methods for feature extraction and description in texture-based image analysis, and more precisely in face recognition.**

In image processing, a **Gabor Wavelet Filter** represents a band-pass linear filter whose impulse response is defined by a harmonic function multiplied by a **Gaussian** function. A **Gabor function** is the mother wavelet of a wavelet transform. The mother wavelet can be transformed into other wavelets in **Gabor filter bank**. Each wavelet, which makes up the **Gabor filter bank**, is used to capture the energy at a specific frequency and a specific direction. These Gabor wavelets provide a complete image representation [12].

By presenting optimal localization properties in both spatial and frequency domain, **Gabor functions** are well suited for texture segmentation, edge detection and image representation problems [13].

The authors, Marcelja [14] and Daugman [15], are the first to advance the idea that **Gabor functions** can be used to model simple cells in the visual cortex of mammalian brains. Thus, image analysis using **Gabor filters** is thought to be similar to perception in the human visual system [12].

A **bi-dimensional Gabor filter** ( $G_{f,\theta}(x,y)$ ) can be viewed as a **Gaussian kernel** function modulated by a sinusoidal plane wave of particular frequency and orientation as follows:

$$G_{f,\theta}(x,y) = e^{-\left[\frac{x_{\theta_n}^2}{\sigma_x^2} + \frac{y_{\theta_n}^2}{\sigma_y^2}\right]} e^{i(2\pi f x_{\theta_n} + \varphi)} \quad (1)$$

where:  $x_{\theta_n} = x \cos \theta_n + y \sin \theta_n$ ,  $y_{\theta_n} = y \cos \theta_n - x \sin \theta_n$ ,  $f$  provides the central frequency of the sinusoidal plane wave at the angle  $\theta_n$ ,  $\sigma_x$  and  $\sigma_y$  represent the standard deviations of the **Gaussian** envelope along the  $X$  and  $Y$  axes.

The filter has two components (Figure 2. ), a real and an imaginary component, representing orthogonal directions:

$$RE_{f,\theta}(x,y) = e^{-\left[\frac{x_{\theta_n}^2}{\sigma_x^2} + \frac{y_{\theta_n}^2}{\sigma_y^2}\right]} \cos(2\pi f x_{\theta_n} + \varphi) \quad (2)$$

$$IM_{f,\theta}(x,y) = e^{-\left[\frac{x_{\theta_n}^2}{\sigma_x^2} + \frac{y_{\theta_n}^2}{\sigma_y^2}\right]} \sin(2\pi f x_{\theta_n} + \varphi) \quad (3)$$



Figure 1. Example of Gabor filter (real and imaginary part)

The **2D filters** define by relation (1), represent a group of wavelets and can optimally capture both local orientation and frequency information from an image. By using  $G_{f,\theta}(x,y)$ , the image is filtered at various orientations, frequencies and standard deviations. Thus, in order to design a **Gabor filter**, we must define the **Phase**, the **Orientations**, the **Frequencies** and **Standard deviations**.

For facial feature extraction, we set the phase to  $\varphi = \frac{\pi}{2}$  and define the angle  $\theta_n$  as:

$$\theta_n = \frac{\pi}{p}(n-1) \quad (4)$$

where,  $p$  denotes the number of orientations and  $n \in \{1 \dots p\}$ .

In this paper for feature extraction we are using the real part of the **Gabor representation**. Thus, being given equations (2) and (4), we consider eight spatial frequencies  $f$ , five orientations  $\theta$  and variance values  $\sigma_x = 2$ ,  $\sigma_y = 1$ . Therefore, the **2D Gabor filter bank** is composed of 40 channels (Figure 2. ).

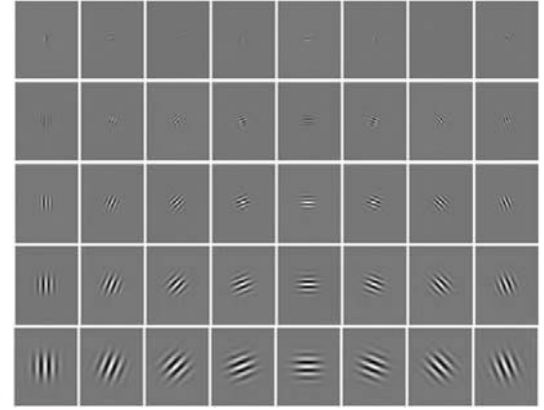


Figure 2. Real part of the used Gabor filters

The **Gabor feature** representation of a grey-scale image  $I(x,y) \in R^{m \times n}$ , where  $m \times n$  represents the image size in pixels, is obtained by convolving the input face image with the created **Gabor filters** (Figure 3. ).

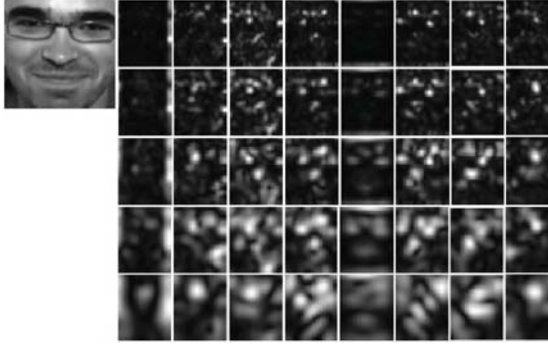


Figure 3. Gabor filter output

### III. NEURAL NETWORKS

In machine learning, *Artificial Neural Networks* represent an information processing paradigm, inspired by the way that biological neural networks process information. In general, they are used to approximate unknown non-linear functions with a large number of inputs. Artificial neural networks are composed of a large number of highly interconnected processing elements, called neurons, which exchange messages between each other. Each connection between two neurons has an adaptive numeric weight assigned. In typical neural networks, the neuron's output is determined by summing all the weighted inputs and feeding them into a function, called activation function.

For a given artificial neuron with  $n$  input signals, the neuron's mathematical functionality is described by:

$$y_k = \varphi(\sum_{j=1}^n w_j x_j + b) \quad (5)$$

where,  $\varphi$  is the neuron's transfer function,  $w_j$  represent the adaptive numeric weights (one for each input signal) and  $b$  the bias value.

Artificial neural networks, like humans, learn by example. This is achieved by tuning the neurons connection weights, making neural nets adaptive to inputs and capable of learning.

In this work, for creating the subject's face model we are using pattern-nets. They represent a special sub-class of feed-forward artificial neural networks (FFANN) that can be trained to classify inputs according to target classes. The main focus of pattern-nets is the recognition of patterns and regularities in data. A FFANN (Figure 4.) usually consists of three neuronal layers: input layer, hidden layer and output layer, each subsequent layer has a connection from the previous one. The final layer (or output layer) produces the network's output. Figure 4. illustrates the architecture of such network; it contains  $n$  input neurons,  $m$  hidden neurons and  $k$  output neurons. Feed-forward ANNs allow signals to travel only one way: from input to output. There is no feedback from the outputs to any other layer.

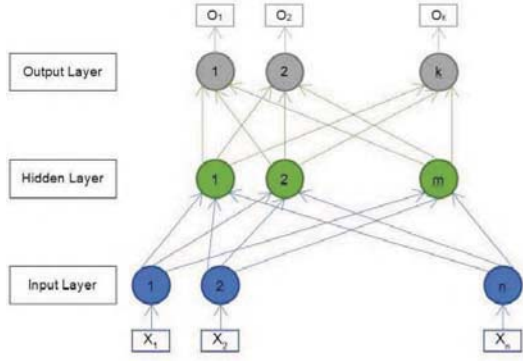


Figure 4. Architecture of Pattern-Net

During the training procedure, the network's output vector  $\mathbf{o}$  (corresponding to an input vector  $\mathbf{x}$ ) is compared with a target vector  $\mathbf{t}$ . The neurons weights and bias values are updated in order to minimize the network's error. The training process ends when the error reaches its minimum or a predefined value.

### IV. PROPOSED ALGORITHM

In this section are described the proposed algorithm's steps; a block diagram of the proposed algorithm is presented in Figure 5. . The algorithm is designed to use *grey-scale* images thus, in case the image is a color one, we convert the *RGB* (red – green – blue) color space to *HSV* (hue – saturation – value) color space and keep the *V* component. Afterwards, each face image from the database is resized to **160x128** pixels.

From the known subject's face image (grey-scale) the feature vector is extracted using a Gabor filters bank at 5 frequencies and 8 orientations; in total **40** filters are used.

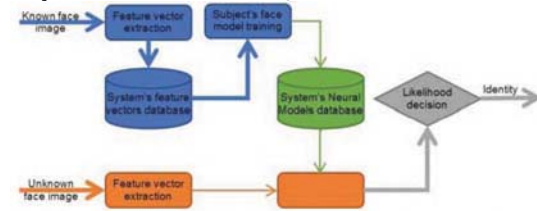


Figure 5. Block diagram of proposed face recognition procedure

The response of each *Gabor kernel filter* is a complex function with a real part and an imaginary part. In this paper we use the magnitude response of the filter  $\|G_{f,\theta}(x,y)\|$  to create the image feature vectors.

$$\|G_{f,\theta}(x,y)\| = \sqrt{\Re^2\{G_{f,\theta}(x,y)\} + \Im^2\{G_{f,\theta}(x,y)\}} \quad (6)$$

where,  $\Re\{G_{f,\theta}(x,y)\} / \Im\{G_{f,\theta}(x,y)\}$  represent the real / imaginary parts of the *Gabor filter*.

The *Gabor features* vector  $x$  is obtained after convolving the face image  $I(x,y)$  with all *Gabor wavelets*  $G_{f,\theta}$  and calculating the magnitudes for all frequencies and orientations. After applying the *Gabor filter bank*, 40 outputs are obtained, each output with the size of **160x128** pixels. Then, each of **40** outputs is down-sampled with a factor of **16** and normalized in order to have zero mean and



unit variance. The feature vector extraction's last step is the concatenation of all previously obtained values into the feature vector  $x$ , resulting of 51200 ( $40 \times 160 \times 128 / 16$ ) values. All feature vectors are stored in order to be used in the neural model training stage.

After the feature vector's extraction, we generate a neural model for each known subject. As mentioned earlier, pattern-nets are used. Each neural network has 51200 inputs, a fixed number of hidden neurons (25 neurons) and two output neurons. The output neurons segment the data in two classes: subject and others. The target data equals 1 for first output neuron in case that the face image belongs to the subject and 0 other wise. The second output neuron is the conjugate of the first.

In the study, hyperbolic tangent sigmoid function is selected as the hidden neuron's transfer function. The tangent hyperbolic function (Figure 6. ) is a bipolar version of the sigmoid function; it produces the scaled output over the -1 to 1 ([16]; [17]).

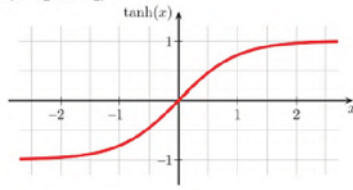


Figure 6. Tan-Sigmoid Transfer function

In the training stage we use as learning algorithm the back-propagation and the *cross-entropy* (CE) as network error function [18]. For each pair of *output-target* elements the cross-entropy is calculated as:  $ce = -t \cdot \log(y)$  (where,  $t$  is the target state and  $y$  represents the networks output). This function heavily penalizes outputs that are extremely inaccurate while offering very little penalty for fairly correct classifications.

In the recognition stage, the unknown face image is processed (RGB to HSV conversion, resizing), then converted to feature vector using the *Gabor filter bank*, and passed as input to all known face models. The subject's identity is selected using a *nearest-neighbor classifier* with the *cosine similarity measure*, applied on the neural networks output.

## V. EXPERIMENTAL RESULTS

All experiments were executed using one color face databases **Caltech 101** [19] and three grey-scale face databases **Yale Face** [20], **Extended Yale B** [21] and **ORL** [22]. The **Caltech** database contains 450 frontal face color images ( $896 \times 592$  pixels) of 26 unique subjects with different lighting, expressions and backgrounds (Figure 7. ). The face regions from the images are extracted using a *Viola-Jones* [23] face detector. Some images have very poor lighting conditions (are too dark or too bright) and were excluded. After the face segmentation more than 200 faces of 26 unique individuals remain.



Figure 7. Sample images from Caltech face database

The **Yale Face** database consists of 11 different grey-scale pictures for 15 unique individuals. The images were acquired with several configurations and facial expressions: normal, center-light, with glasses, happy, left-light, no glasses, right-light, sad, sleepy, surprised, and wink (Figure 8. ).



Figure 8. Sample images from Yale face database

The extended **Yale Face Database B** contains 16128 grey-scale images of 28 human subjects under 9 poses and 64 illumination conditions, resulting 576 viewing conditions for every subject. The images are aligned, cropped and resized. The nine poses recorded are as following: pose 0 is the frontal pose; poses 1, 2, 3, 4, and 5 were about 12 degrees from the camera optical axis, while poses 6, 7, and 8 were about 24 degrees. In this paper, only a subset of the database was used, consisting of 63 pictures per subject under the following conditions: nine poses (0 to 8), five azimuth positions (0, +0.5, -0.5, +1, -1 degrees) and three elevation positions (0, +10, -10 degrees) (see Figure 9. ).



Figure 9. Sample images from Yale B face database

The **ORL** (Olivetti Research Laboratory) face database contains a set of gray-scale faces taken between April 1992 and April 1994. There are 10 different images of 40 distinct subjects. The images were taken at different times, varying slightly, facial expressions (open / closed eyes, smiling / non-smiling) and facial details (glasses/no-glasses). All the images are taken against a dark homogeneous background and the subjects are in up-right, frontal position.



Figure 10. Sample images from ORL face database

For our algorithm testing, the databases were divided in two parts: first one contains 4 random selected pictures per subject and was used to generate the face model; the second one consists of the remaining facial pictures and was used as test data. For each database we repeated the experiments 5 times on random train and test image sets; afterwards we measured the effectiveness of the proposed algorithm using several standard error and recognition rates. For each of the five validation experiments, we computed four rates:

- the first rate is rank one recognition rate (**ROR**)
- the false acceptance rate (**FAR**), indicates the percentage of accepted non-authorized users;
- the false rejection rate (**FRR**), indicates the percentage of incorrectly rejected authorized users;
- the minimal half total error rate (**mHTER**) [24]:

$$mHTER = \min \left( \frac{FAR + FRR}{2} \right) \quad (7)$$

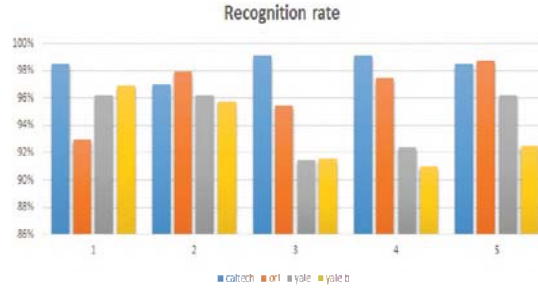


Figure 11. System Recognition rate

TABLE I. SYSTEM RECOGNITION RATE

	Database			
	Caltech	ORL	Yale	Yale B
Min	96.99%	92.92%	91.43%	91.01%
Max	99.10%	98.75%	96.19%	96.94%
Mean	98.43%	96.50%	94.48%	93.53%

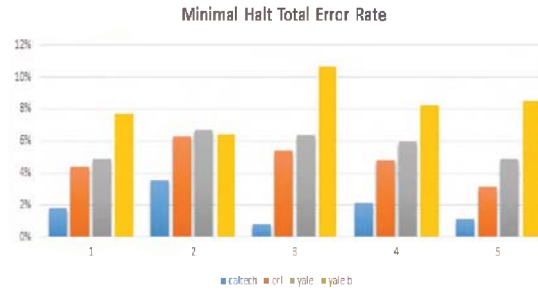


Figure 12. System mHTER

TABLE II. SYSTEM mHTER

	Database			
	Caltech	ORL	Yale	Yale B
Min	0.80%	3.13%	4.90%	6.41%
Max	3.51%	6.26%	6.70%	10.63%
Mean	1.87%	4.80%	5.76%	8.29%

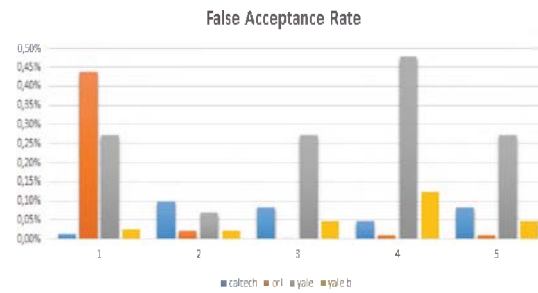


Figure 13. System FAR at mHTER

TABLE III. SYSTEM FAR AT MHTEP

	Database			
	Caltech	ORL	Yale	Yale B
Min	0.01%	0.00%	0.07%	0.02%
Max	0.10%	0.44%	0.48%	0.12%
Mean	0.07%	0.10%	0.27%	0.05%



Figure 14. System FRR at mHTER

TABLE IV. SYSTEM FRR AT MHTEP

	Database			
	Caltech	ORL	Yale	Yale B
Min	1.51%	6.25%	9.52%	12.80%
Max	6.93%	12.50%	13.33%	21.22%
Mean	3.67%	9.50%	11.24%	16.53%

In order to compare the average recognition rate of our algorithm, using the same sets of images, we trained and tested different classical face recognition algorithms [25] [26]:

- Gabor - PCA and the nearest neighbor classifier;
- Gabor - LDA and the nearest neighbor classifier;
- Gabor - KFA and the nearest neighbor classifier.
- Gabor - KPCA and the nearest neighbor classifier.

The results of our experiments are presented in TABLE V. to TABLE VIII.

TABLE V. RECOGNITION RATE COMPARISON

	Caltech	ORL	Yale	Yale B	Mean
Own	98.43%	96.50%	94.48%	93.53%	95.74%
PCA	97.95%	90.58%	87.62%	90.66%	91.70%
LDA	98.73%	98.33%	95.62%	97.88%	97.64%
KFA	99.04%	97.33%	87.05%	98.75%	95.54%
KPCA	94.34%	87.33%	52.00%	84.51%	79.54%

TABLE VI. MHTEP COMPARISON

	Caltech	ORL	Yale	Yale B	Mean
Own	1.87%	4.80%	5.76%	8.29%	5.18%
PCA	0.53%	0.46%	1.30%	0.75%	0.76%
LDA	0.34%	0.39%	0.95%	0.59%	0.57%
KFA	0.34%	0.70%	4.56%	0.38%	1.50%
KPCA	0.88%	0.49%	21.59%	1.76%	6.18%

TABLE VII. FAR AT MHTEP COMPARISON

	Caltech	ORL	Yale	Yale B	Mean
Own	0.07%	0.10%	0.27%	0.05%	0.12%
PCA	0.28%	0.40%	1.46%	0.78%	0.73%
LDA	0.26%	0.33%	1.70%	0.62%	0.73%
KFA	0.14%	0.59%	3.80%	0.31%	1.21%
KPCA	0.86%	0.52%	20.33%	1.32%	5.76%

TABLE VIII. FRR AT MHTEP COMPARISON

	Caltech	ORL	Yale	Yale B	Mean
Own	3.67%	9.50%	11.24%	16.53%	10.24%
PCA	0.78%	0.58%	1.14%	0.72%	0.81%
LDA	0.42%	0.50%	0.19%	0.56%	0.42%
KFA	0.54%	0.75%	5.33%	0.45%	1.77%
KPCA	0.90%	0.58%	22.86%	2.20%	6.64%

## VI. CONCLUSION

In this paper, we have presented a *novel hybrid algorithm* for face identification / recognition by *combining Gabor-based features* with *Neural Networks*. When analyzing the system recognition rate (*ROR* - TABLE V. ), we can see that the new hybrid method outperforms three of the classical face recognition algorithms described by Štruc and Pavasi [25] [26]. TABLE V. proves the effectiveness of the proposed algorithm, only one, out of the four the classical face recognition algorithms, presents a *ROR* with *1.9%* higher.

Using a small number of training images per subject, the proposed system managed to achieve over *95% recognition rate*.

TABLE V., *ROR* comparison, shows that the classical approaches are heavily influenced by the different facial expressions and poses. The results obtained on the *Yale* and *Yale B* database, the recognition rate of the classical systems drop by as much as *40%*, from *94.34%* till *52%* (*KPCA method*). The new hybrid algorithm presented a degradation smaller the *4%*.

Having a high recognition rate, over *95%*, and a very small "*False Acceptance Rate*" (TABLE VII. ), less than *0.5%*, the proposed method is ideal for face verification systems.

For this paper, the total number of neurons, of the neural network used to generate the subject face model, was determined by trial and error. We must continue our experiments, in order to determine the optimal number of neurons contained in the network, and also to check if there exists a correlation between the number of neurons and the number of subjects.

## REFERENCES

- [1] Acuity Market Intelligence, "The Global Biometrics and Mobility Report: The Convergence of Commerce and Privacy," 2016.
- [2] R. Jafri and H. R. Arabnia, "A Survey of Face Recognition Techniques," *Journal of Information Processing Systems*, vol. 5, no. 2, pp. 41-67, 2009.
- [3] F. G. Filip, B.-C. Zamfirescu and C. Ciurea, Computer-Supported Collaborative Decision-Making, Springer International Publishing, 2017.
- [4] Amscreen, "Amscreen to launch OptimEyes advertising platform," [Online]. Available: <https://www.amscreen.eu/amscreen-to-launch-optimeyes-advertising-platform-2/>. [Accessed 24 03 2019].

- [5] J. Yang, D. Zhang, A. F. Frangi and J.-y. Yang, "Two-dimensional PCA: A new approach to appearance-based face representation and recognition," *IEEE Transactions on Pattern Analysis and Machine Intelligence*, vol. 26, no. 1, pp. 131 - 137, 2004.
- [6] L.-F. Chen, H.-Y. M. Liao, M.-T. Ko, J.-C. Lin and G.-J. Yu, "A new LDA-based face recognition system which can solve the small sample size problem," *Pattern Recognition*, vol. 33, no. 10, pp. 1713 - 1726, 2000.
- [7] B. A. Draper, K. Baek, M. S. Bartlett and J. Beveridge, "Recognizing faces with PCA and ICA," *Computer Vision and Image Understanding*, vol. 91, no. 1-2, pp. 115 - 137, 2003.
- [8] Z. Lei, S. Liao, M. Pietikäinen and S. Z. Li, "Face recognition by exploring information jointly in space, scale and orientation," *IEEE Transactions on Image Processing*, vol. 20, no. 1, pp. 247 - 256, 2011.
- [9] M. Zhou and H. Wei, "Face Verification Using Gabor Wavelets and AdaBoost," in *18th International Conference on Pattern Recognition*, Hong Kong, 2006.
- [10] K. B. Vinay and B. S. Shreyas, "Face Recognition Using Gabor Wavelets," in *Fortieth Asilomar Conference on Signals, Systems and Computers*, 2006.
- [11] D. Gabor, "Theory of communication," *Journal of the Institution of Electrical Engineers - Part III: Radio and Communication Engineering*, pp. 429-457, 1946.
- [12] T. S. Lee, "Image representation using 2D Gabor wavelets," *IEEE TRANSACTIONS ON PATTERN ANALYSIS AND MACHINE INTELLIGENCE*, vol. 18, no. 10, pp. 959-971, 1996.
- [13] T. P. Weldon, W. E. Higgins and D. F. Dunn, "Gabor filter design for multiple texture segmentation," *Optical Engineering*, pp. 2852-2863, 1996.
- [14] S. Marčelja, "Mathematical description of the responses of simple cortical cells," *Journal of the Optical Society of America*, vol. 70, no. 11, p. 1297-1300, 1980.
- [15] J. G. Daugman, "Uncertainty relation for resolution in space, spatial frequency, and orientation optimized by two-dimensional visual cortical filters," *Journal of the Optical Society of America*, pp. 1160-1169, 1985.
- [16] D. L. Civco, "Artificial neural networks for land-cover classification," *International Journal of Geographical Information Systems*, vol. 7, no. 2, pp. 173-186, 1993.
- [17] E. J. Kaminsky, H. Barad and W. Brown, "Textural neural network and version space classifiers for remote sensing," *International Journal of Remote Sensing*, vol. 18, no. 4, pp. 741-762, 1997.
- [18] D. P. Kroese, R. Y. Rubinstein and T. Taimre, "Application of the cross-entropy method to clustering and vector quantization," *Journal of Global Optimization*, vol. 37, no. 1, pp. 137-157, 2007.
- [19] M. Weber, "A frontal face dataset collected by Markus Weber at California Institute of Technology," 1999. [Online]. Available: [http://www.vision.caltech.edu/Image\\_Datasets/faces/faces.tar](http://www.vision.caltech.edu/Image_Datasets/faces/faces.tar).
- [20] P. N. Bellhumer, J. P. Hespanha and D. J. Kriegman, "Eigenfaces vs. fisherfaces: Recognition using class specific linear projection," *IEEE Transactions on Pattern Analysis and Machine Intelligence*, vol. 17, no. 7, pp. 711-720, 1997.
- [21] A. S. Georgiades, P. N. Belhumeur and D. J. Kriegman, "From Few to Many: Illumination Cone Models for Face Recognition under Variable Lighting and Pose," *IEEE Transactions on Pattern Analysis and Machine Intelligence*, vol. 23, no. 6, pp. 643-660, 2001.
- [22] F. S. Samaria and A. Harter, "Parameterisation of a stochastic model for human face identification," *Proceedings of 2nd IEEE Workshop on Applications of Computer Vision*, pp. 138 - 142, 1994.
- [23] P. Viola and M. Jones, "Rapid object detection using a boosted cascade of simple features," *Computer Vision and Pattern Recognition*, vol. 1, pp. 511-518, 2001.
- [24] F. Mihelič and J. Žibert, "Robust speech detection based on phoneme recognition features," in *Lecture Notes in Computer Science*, 2006, pp. 755 - 462.
- [25] V. Štruc and N. Pavesic, "Gabor-Based Kernel Partial-Least-Squares Discrimination Features for Face Recognition," *Informatica*, vol. 20, no. 1, pp. 115-138, 2009.
- [26] V. Štruc and N. Pavesic, "The Complete Gabor-Fisher Classifier for Robust Face Recognition," *EURASIP Journal on Advances in Signal Processing*, p. 26, 2010.